Biometric Authentication via Oculomotor Plant Characteristics

Oleg V. Komogortsev
Texas State University
San Marcos, TX
ok11@txstate.edu

Alex Karpov
Texas State University
San Marcos, TX
Ak26@txstate.edu

Larry R. Price
Texas State University
San Marcos, TX
lprice@txstate.edu

Cecilia Aragon
University of Washington
Seattle, WA
aragon@uw.edu

Abstract

A novel biometrics approach that performs authentication via the internal non-visible anatomical structure of an individual human eye is proposed and evaluated. To provide authentication, the proposed method estimates the anatomical characteristics of the oculomotor plant (comprising the eye globe, its muscles and the brain's control signals). The estimation of the oculomotor plant characteristics (OPC) is achieved by analyzing the recorded eye movement trajectories via a 2D linear homeomorphic mathematical representation of the oculomotor plant. The derived OPC allow authentication via various statistical methods and information fusion techniques. The proposed authentication method yielded Half Total Error Rate of 19% for a pool of 59 recorded subjects in the best case. The OPC biometric authentication has high counterfeit resistance potential, because it includes both behavioral and physiological human attributes that are hard to reproduce.

1. Introduction

The methods of biometric identification have evolved throughout history from basic measurements of head dimensions [1] to more advanced techniques involving fingerprints [2], iris [3], and face recognition [4]. But the above-mentioned techniques are not completely fraud-proof since they are based on human body characteristics that can be replicated with modern technological advances [2-5]. As a result there is a significant need in biometrics research to identify methods that are highly counterfeit resistant. In this paper we present a method that has potential to be highly counterfeit resistant because it employs non-visible anatomical structures of the human eye.

The human eye already provides a plethora of information useful for biometrics. The physical and behavioral properties of the eye are employed in biometrics based on the iris [6], face recognition [4], retina [7], periocular information [8], recordings of the raw eye position, velocity signal and pupil dilation [9, 10].

In terms of its anatomical structure, the eye provides a unique opportunity for identification by containing a multitude of anatomical components that together comprise the so-called *oculomotor plant* (OP). These components are the eye globe and its surrounding tissues, ligaments, six extraocular muscles each containing thin and thick filaments, tendon-like components, various tissues and liquids [11] (Figure 1). The dynamic and static characteristics of the OP are represented by the eye globe's inertia, dependency of an individual muscle's force on its length and velocity of contraction, resistive properties of the eye globe, muscles and ligaments, frequency characteristics of the neuronal control signal sent by the brain to the extraocular muscle and the speed of propagation of this signal. Individual properties of the extraocular muscles vary depending on the role each muscle performs. There are two roles: the agonist - muscle contracts and pulls the eye globe in the required direction and the antagonist - muscle expands and resists the pull [12].

Numerical estimation of the OP characteristics (OPC) could yield a highly counterfeit resistant biometric method because OPC represent dynamic behavioral and physiological human attributes that only exist in a living individual. Biometric authentication via OPC promises to be highly repeatable because any type of random stimulus ideally would produce the same OPC values.

Accurate estimation of the OPC is challenging due to the secluded nature of the corresponding anatomical components, which necessitates indirect estimation and includes noise and inaccuracies associated with the eye tracking equipment, classification and filtering of the eye movement signal, mathematical representation of the OP, and actual algorithms for numerical estimation of the OPC. Eye movement databases that can be readily employed for the evaluation of the OPC biometrics are not available. This work proposes initial solutions to these challenges, records several strictly defined eye movement datasets, and establishes a very thorough performance baseline for OPC biometrics to facilitate future research for this identification modality.

This paper is organized as follows: section 2 presents an overview of biometric authentication via OPC and describes the required architectural components, section 3 presents data recording and evaluation procedures, section 4 presents the results, section 5 provides discussion including the limitations of the OPC biometrics, and section 6 presents conclusions and describes the directions of future work.

2. Biometric Authentication via Oculomotor Plant Characteristics (OPC)

2.1. Overview

The developed architecture presented by Figure 2 allows estimating oculomotor plant characteristics (Figure 1) via recorded eye movement signal (e.g., Figure 3) and creating a unique OPC template (e.g., Figure 4) that is employed during the user's enrollment and verification.

During the enrollment, the recorded eye movement signal from an individual is supplied to the Eye Movement Classification module that classifies the eye position signal into fixations (movements that keep an eye focused on a stationary object of interest) and saccades (extremely rapid eye rotations between the points of fixation). OPC can be extracted only from a dynamic eye movement such as saccade. Therefore, a sequence of classified saccades' trajectories is sent to the second module labeled Oculomotor Plant Mathematical Model (OPMM), which generates simulated saccades' trajectories based on the default OPC values that are grouped into a vector with the purpose of matching the simulated trajectories with the recorded ones. Each individual saccade is matched independently of any other saccade. Both classified and simulated trajectories for each saccade are sent to the Error Function module where the error between the trajectories is computed. The error result triggers the OPC Estimation, module to optimize the values inside of the OPC vector minimizing the error between each pair of recorded and simulated saccades. When the minimum error is achieved for all classified and simulated saccade pairs an OPC biometric template representing a user is generated. The template consists of a set of the optimized OPC vectors, with each vector representing a classified saccade. The number of classified saccades essentially determines the size of the user's OPC biometric template.

During a person's verification, the information flow is similar to the enrollment procedure. In addition, the estimated user biometrics template is supplied to the Person Authentication and Information Fusion modules to authenticate a user. The Person Authentication module accepts or rejects a user based on the recommendation of a given classifier. The Information Fusion module aggregates information related to OPC vectors and works with the Person Authentication module to authenticate a person based on multiple classification methods. The output during user authentication procedure is a yes/no answer about claimed user's identify.

Detailed description for each module is provided next.

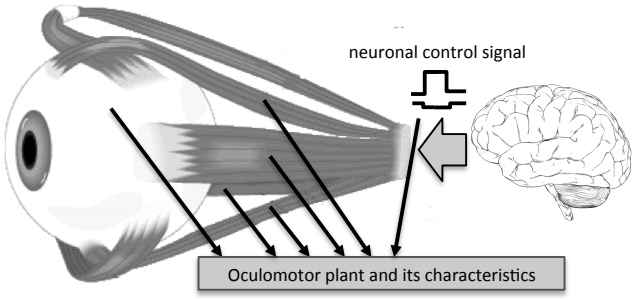

Figure 1: Oculomotor plant characteristics.

2.2. Eye Movement Classification

An automated eye movement classification algorithm plays a crucial role in aiding the establishment of the invariant representation for the subsequent estimation of the OPC values. The goal of this algorithm is to automatically and reliably identify each saccade's beginning, end and all trajectory points from a very noisy and jittery eye movement signal (e.g. Figure 3). Another goal of the eye movement classification algorithm is to provide additional filtering for saccades to ensure their high quality and a sufficient quantity of data for the estimation of the OPC values.

A standardized Velocity-Threshold (I-VT) algorithm [13] was selected due to its speed and robustness. A comparatively high classification threshold of 70°/s is employed to reduce the impact of trajectory noises at the beginning and the end of each saccade. Additional filtering discarded saccades with amplitudes of less than 4°/s, dura-

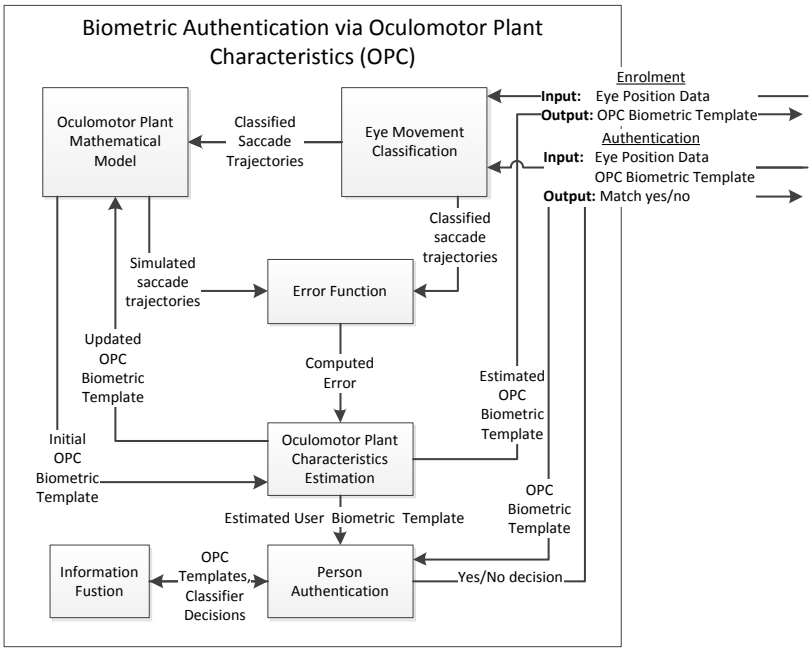

Figure 2: Architecture for the biometric authentication via oculomotor plant characteristics.

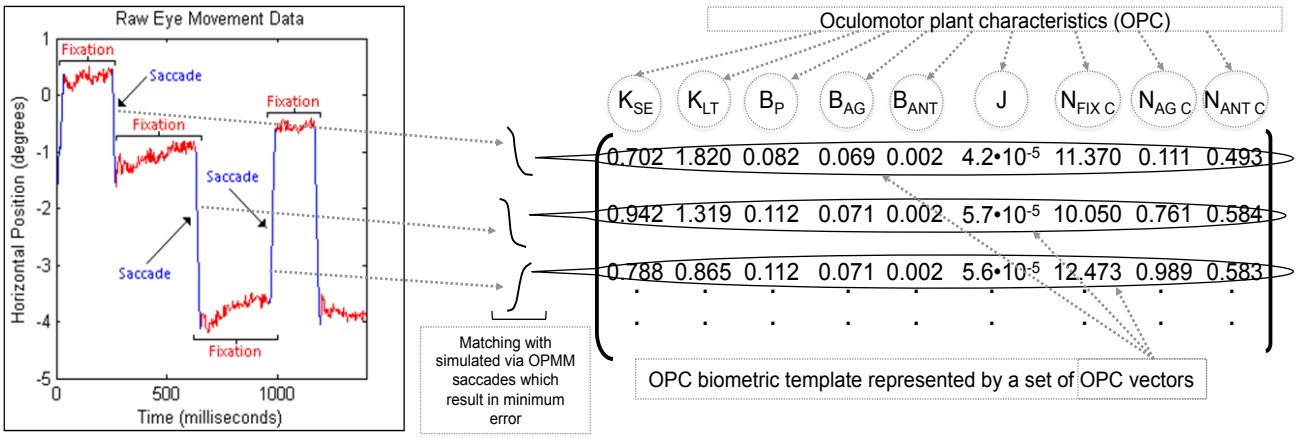

Figure 3: Raw eye movement signal with classified fixations and saccades (Left). OPC biometric template (Right). In the middle simulated via OPMM saccade trajectories generated with the OPC vectors that provide the closest match to the recorded trajectories are presented.

tion of less than 20 ms., and various trajectory artifacts that do not belong to normal saccades.

2.3. Oculomotor Plant Mathematical Model

The OPMM has to be able to quickly simulate accurate saccade trajectories while containing major anatomical components related to the OP.

The linear homeomorphic 2D OP mathematical model developed by Komogortsev and Jayarathna [14] is selected. This OPMM, driven by twelve differential equations, is capable of simulating saccades with properties resembling normal humans on a 2D plane (e.g. computer monitor) by considering physical properties of the eye globe and four extraocular muscles: medial, lateral, superior, and inferior recti. The following advantages are associated with a selection of this OPMM: 1) major anatomical components are accounted for and can be estimated, 2) linear representation simplifies the estimation process of the OPC while producing accurate simulation data within the spatial boundaries of a regular computer monitor, 3) the architecture of the model allows dividing it into two smaller 1D models of the form that is described by Komogortsev and Khan [12]. One of the smaller models becomes responsible for the simulation of the horizontal component of movement and the other for the vertical. Such assignment, while producing identical simulation results when compared to the full model, allows a significant reduction in the complexity of the required solution and allows simultaneous simulation of both movement components on a multi-core system.

A detailed description of the model is beyond the scope of this paper and can be found in [14]. Specific OPC accounted by the OPMM and selected to be a part of the user's biometric template are discussed next.

2.4. OPC vector

The following subset of nine OPC was empirically selected (Figure 3) as a vector to represent an individual saccade for each component of movement (horizontal and vertical). *Length tension* (K_{lt}=1.2 g/°)[1] - the relationship between the length of an extraocular muscle and the force it is capable of exerting, *series elasticity* (K_{se}=2.5 g/°) - resistive properties of an eye muscle while the muscle is innervated by the neuronal control signal, *passive viscosity* (B_p=0.06 g·s/°) of the eye globe, *force velocity relationship* - the relationship between the velocity of an extraocular muscle extension/contraction and the force it is capable of exerting - in the agonist muscle (B_{AG}=0.046 g·s/°), *force velocity relationship* in the antagonist muscle (B_{ANT}=0.022 g·s/°), agonist and antagonist muscles' *tension intercept* (N_{FIX_C}=14.0 g) that ensures an equilibrium state during an eye fixation at primary eye position, the agonist muscle's *tension slope* (N_{AG_C}=0.8 g), and the antagonist muscle's *tension slope* (N_{ANT_C}=0.5 g), *eye globe's inertia* (J=0.000043 g·s^2/°). All tension characteristics are directly impacted by the neuronal control signal sent by the brain and therefore partially contain the neuronal control signal information.

The remaining OPC to produce the simulated saccades are fixed to the following default values: agonist muscle neuronal control signal activation (11.7) and deactivation constants (2.0), antagonist muscle neuronal control signal activation (2.4) and deactivation constants (1.9), pulse height of the antagonist neuronal control signal (0.5 g), pulse width of the antagonist neuronal control signal (PW_{AG}=7+|A| ms.), passive elasticity of the eye globe (K_p= N_{AG_C} – N_{ANT_C}) pulse height of the agonist neuronal control signal (iteratively varied to match recorded saccade's onset and offset coordinates), pulse width of the agonist neuronal control signal (PW_{ANT}= PW_{AG}+6).

2.5. Error Function

The goal of the Error Function module is to provide high sensitivity to any differences between the recorded and simulated saccade trajectories.

[1] Numbers in brackets represent default values. Following notations are employed g – grams, s – seconds, ° - degrees of the visual angle, A – amplitude of the recorded saccade.

The error function is implemented as the absolute difference between the saccades that are recorded by an eye tracker and saccades that are simulated by the OPMM.

$$R = \sum_{i=1}^{n} |t_i - s_i| \quad \textbf{(1)}$$

where n is the number of points in a trajectory, t_i is a point in a recorded trajectory and s_i is a corresponding point in a simulated trajectory. The absolute difference approach provides an advantage over other estimations such as root mean squared error (RMSE) due to its higher absolute sensitivity to the differences between the saccade trajectories.

2.6. OPC Estimation & Biometric Template

The goal of the OPC estimation module is to provide a mechanism for optimizing the values in the OPC vector to ensure a minimum error between the simulated and recorded saccade trajectories. The resulting optimum OPC vectors create the OPC biometric template for a given user (Figure 3).

The Nelder-Mead (NM) simplex algorithm [15] (fminsearch implementation in MATLAB) is used in a form that allows simultaneous estimation of all OPC vector parameters at the same time. Lower and upper boundaries are imposed to prevent reduction or growth of each individual OPC value to less than 10% or larger than 1000% of its default value. Stability degradation of the numerical solution for differential equations describing the OPMM is used as an additional indicator for acceptance of the suggested OPC values by the estimation algorithm.

2.7. Person Authentication

The goal of the Person Authentication module is to confirm or reject claimed identity based on the comparison of the two OPC biometric templates.

One of the biggest challenges associated with the OPC biometrics is the amount of variability present in the estimated OPC. Experiments from which one might infer the variability of OPC values are almost non-existent in the OP literature. Usually, average numbers are derived from strabismus surgeries performed on a limited number of patients [16], and even from cat studies [17]. As a result it is hard to estimate a priori the amount of variability of the values for the OP properties in a large pool of normal humans. We hypothesize that a substantial amount of variability is present in the OPC to ensure accurate authentication. Therefore, authentication methods that allow addressing variability concerns are required to make OPC biometrics successful.

Two classifiers fit this purpose: a) Student's *t*-test [18] enhanced by voting and b) Hoteling's *T*-square test [19]. Both methods are able to perform acceptance and rejection tests. In the acceptance test, two OPC biometric templates each in a form of a set of OPC vectors belonging to the same individual are compared. In the rejection test, the templates are taken from different people. The outcome of each test determines the authentication accuracy of the corresponding authentication approach.

2.7.1 Student's t-test with Voting

The following Null Hypothesis (H_0) is formulated as a part of the Student's *t*-test given that two biometric templates, one from the user *i* and the other from the user *j*, are compared: "H_0: There is no difference between the templates from the users *i* and *j*". In order to make a conclusion about the difference between two users, the statistical significance (p_{level}) resulting from the test is compared to the significance threshold α. If the resulting p_{level} is smaller than α, the H_0 is rejected indicating that the templates belong to different people. Otherwise, the H_0 is accepted indicating that the templates belong to the same person.

The Student's *t*-test approach allows performing an authentication based on a template that contains information about single OPC, therefore not taking immediate advantage of the potential information included in other OPC. In this work we enhance the Student's *t*-test by considering voting methods described by Lam and Suen [20]. This method accepts a person assuming that for at least *k* OPC the H_0 is accepted and rejects a person if H_0 is accepted for less than *k* OPC. The performance of the Student's *t*-test with voting is affected by the significance threshold and number of votes *k*. Voting allows to disregard OPC that might violate normality requirement imposed by the Student's *t*-test.

2.7.2 Hotelling's T-square Test

Hotelling's *T*-square test [19] is a multivariate representation of the Student's *t*-test and therefore provides a test of the multivariate distribution for the entire OPC vector in a template rather than evaluating parameters in an "isolated" or "single" approach where only one OPC is considered. Hotelling's *T*-square is well-suited for assessing the performance of OPC biometric authentication across all parameters because the true significance level of the *T*-square test is most sensitive to mean differences resulting from more than one measurement occasion (or experimental condition) and is less affected by discrepancies between the covariance matrices attributable to different people (or experimental conditions) - as long as the sample sizes used are large (e.g., number of subject $N \geq 40$ or number of samples $n \geq 10$ in each experimental condition [21]). Number of samples can be interpreted as the number of recorded saccades in case of the OPC biometrics.

2.8. Information Fusion

Information fusion techniques allow improvement of the overall accuracy of an authentication method by considering the information from multiple classifiers [22].

A decision level fusion technique proposed by Daug-

man in a form of AND/OR approach [23] was employed to combine the decisions of multiple classifiers and vertical/horizontal movement components. For simplicity we call this method *logical fusion*. The AND method only accepts an individual if all of the classifiers accept the individual, therefore providing an opportunity to reduce the combined false acceptance rate and increase the resulting false rejection rate. The OR method only accepts an individual if one of the classifiers accepts the individual, therefore providing an opportunity to increase the combined false acceptance rate and decrease the combined false rejection rate.

3. Experimental Setup

3.1. Apparatus & Software

The data was recorded using the EyeLink 1000 eye tracker with a sampling frequency of 1000Hz [24]. The EyeLink 1000 provides drift free eye tracking with a spatial resolution of 0.01º, and 0.25-0.5º of positional accuracy. EyeLink 1000 enables eye to camera distances between 60 and 150cm and horizontal and vertical operating range of 55° and 45° respectively. To ensure high accuracy of the eye movement recording a chin rest was employed. The chin rest was positioned to assure 70cm distance between the display surface and the eyes of the subject. The OPC biometrics architecture was implemented in MATLAB. All data was processed offline.

3.1. Participants

A total of 59 participants (46 males/13 females), ages 18 – 45 years with an average age of 24 (SD=6.1), volunteered for the project. Mean positional accuracy of the recordings averaged between all screen regions was 1.41º (SD=1.91º).

All subjects participated in the two recording sessions that presented identical eye movement invocation tasks with approximately a 20 minute break between the sessions. Before each recording session, for each subject and eye movement invocation task, the eye tracking equipment was recalibrated to ensure high positional accuracy of the recorded data.

3.2. Stimuli & Resulting Datasets

The goal of the stimulus was to invoke a large number of vertical and horizontal saccades to allow reliable authentication. The stimulus was displayed as a jumping dot, consisting of a grey disc sized approximately 1º with a small black point in the center. The dot performed 100 jumps horizontally and 100 jumps vertically.

The amplitude of the vertical jumps was 20º for all subjects. However, horizontal jumps had the amplitude of 20º for approximately half of the subjects (27) and 30º for another half (32). The variation in the horizontal amplitudes allowed assessing classification performance due to stimulus changes while fixed vertical amplitude allowed testing for the scalability of the OPC biometrics for a larger pool of individuals.

The horizontal component of movement from horizontal saccades with 20º amplitude and the vertical component of movement from the vertical saccades with 20º amplitude obtained from first 27 subjects comprised Dataset I. The horizontal component of movement from horizontal saccades with 30º amplitude and the vertical component of movement from the vertical saccades with 20º amplitude recorded from the remaining 32 subjects comprised Dataset II. Dataset I+II combined data from datasets I and II. All datasets are publically available as a part of the Eye Movement Biometrics Database v1 [25].

The use of just horizontal movement components from purely horizontal saccades and vertical component from purely vertical saccades allows substantial improvement of the quality of data employed for authentication by disregarding orthogonal movement jitter. If necessary, such eye movement data allows a subsequent check for saccade normality by filtering via the corresponding amplitude-duration and amplitude- maximum velocity relationships (main-sequence relationship) [26] and discard outliers. However, the filtering based on the two above mentioned relationship was not performed and currently remains a goal of the future work. All datasets provide necessary amount of subjects and number of recorded saccades for application of Hotelling's *T*-square test and Student's *t*-test.

Data quality for Dataset I+II: Mean positional accuracy averaged between all screen regions is 1.25º (SD=1.45º). Average amount of the invalid data (eye positional samples not properly detected by the eye tracker) is 3.16% (SD=5.34%). Average behavioral scores as defined in [13] when the raw eye positional data is separated into the fixations and saccades by the I-VT algorithm with a threshold of 70º/s are: SQnS=108% (SD=50%), FQnS=58% (SD=14.7%), and the FQlS=0.95º (SD=0.42º).

4. Results

Data analysis: All nine OPC parameters for all datasets were screened for multivariate normality and homogeneity covariance matrices. Six of the nine parameters displayed a continuous normal distribution although excessive positive skewness and kurtosis were observed. However, the degree of skewness and kurtosis was not extreme to the degree that the data required a transformation given the robust characteristics of Hotelling's *T*-square test to violations of normality [27]. The distribution displayed by K_{se}, B_{ANT}, and N_{ANT_C} OPCs was Negative Binomial [28] and subsequently required a logarithmic transform prior to analysis.

Method & Data Description		Selection	Best			Fixed		
		Dataset	I	II	I+II	I	II	I+II
1	T(hor)		18.5	26	23	26	28.5	24.5
2	T(ver)		25.5	28	26	28.5	35.5	32.5
3	S(hor)		19	24	21.5	24.5	30.5	25
4	S(ver)		23	28	29.5	36.5	34.5	40.5
5	T(hor) *OR* S(hor)		18.5	24.5	20.5	22	29	26
6	T(ver) *OR* S(ver)		22	24.5	25	29.5	34	34.5
7	T(hor) *OR* T(ver)		19	18.5	19	26	22.5	22.5
8	S(hor) *OR* S(ver)		19	21.5	22.5	31.5	31	25.5
9	T(hor) *AND* S(hor)		16	28	23	25.5	28.5	24.5
10	T(ver) *AND* S(ver)		26	28	26	27	35.5	32
11	T(hor) *AND T*(ver)		24	38.5	36.5	27.5	41	33.5
12	S(hor) *AND* S(ver)		22	24.5	24	31	30.5	28

Table I. Performance of the OPC biometrics for various authentication methods and datasets expressed in the HTER (numbers show percentages). In the Methods & Data Description column T represents Hotelling's *T*-square test and S represents Students *t*-test with voting. (hor) represents data from horizontal movement component of horizontal saccades, (ver) represents data from vertical movement of vertical saccades. OR and AND represent logical fusion techniques. Note that for "Fixed" results related to Students *t*-test with voting represent values obtained with 3 votes (7 votes in case of horizontal fusion). Significance threshold α for Students *t*-test and Hotelling's *T*-square test was 0.1. For "Best" results the optimal number of votes (ranging from 1 to a total number of OPC used in authentication vector) and significance threshold (ranging from 0.1 to 0.9) was selected.

Authentication Performance: Table I presents performance results. Half Total Error Rate (HTER) metrics as defined in [22] is employed for the assessment of the authentication accuracy. "Best" tab presents highest authentication accuracy afforded by selection of an optimal OPC subset for each authentication method, significance threshold and number of votes in the Student's *t*-test. Optimal OPC subset can vary for different cases. "Fixed" tab presents authentication results for a fixed subset of OPC that remains invariant for all authentication methods. "Fixed" approach allows assessing the stability of the OPC biometrics, and indicates accuracy of performance during more practically applicable scenario of use. To select the fixed OPC subset principal component analysis (PCA) was performed on nine OPC that comprise an OPC vector in an effort to reduce the number of parameters needed for the authentication. Results of PCA indicate that series elasticity (K_{se}), passive viscosity of the eye globe (B_p), eye globe's inertia (J), agonist muscle's tension slope (N_{AG_C}), and the antagonist muscle's tension slope (N_{ANT_C}) account for 77% of total variance in the recorded data. These parameters were selected to represent fixed OPC subset.

4.1. "Fixed" Performance

4.1.1 Impact of Person Authentication Methods

As shown in rows 1-4 in Table I, Hotelling's *T*-square test in general produced slightly more accurate authentication results than Student's *t*-test with voting for most of datasets under consideration. For example, in Dataset I+II, the Hotelling's *T*-square test produced HTER of 24.5% for horizontal while Student's *t*-test with voting produced HTER of 25%. For vertical data the difference between tests was 8%.

4.1.2 Impact of Logical Fusion Impact

According to rows 5-12 in Table I, application of logical fusion has a capability to provide an increase in the authentication accuracy when compared to pure person authentication methods. For example, in Dataset I+II, Hoteling's *T*-square test for the horizontal component produced HTER of 24.5% and for the vertical component produced HTER of 32.5%; however, logical fusion reduced the HTER to 22.5% (row 7).

4.1.3 Impact of Stimuli Properties

The results from horizontal data presented in row 1 and 3 of Table I indicate lower authentication accuracy for the saccades of larger amplitudes. We hypothesize that such phenomena can be explained by the increased amount of express saccades and also undershoots and overshoots [26] that occur as a part of the person's reaction to the large amplitude stimuli.

For the Dataset I+II, where different stimulus amplitudes were used for different subject groups, the accuracy of authentication was better than the average of HTERs produced by each dataset separately.

Both results suggest that stimulus amplitude does impact the results of biometric authentication, however slightly. Additional research is required to provide an additional clarification.

4.1.4 Scalability of the OPC biometrics

The results from the vertical data presented in row 2 and 4 of the Table I indicate the scalability potential of the OPC biometrics, because such data considers saccades recorded in a response to the same stimulus amplitude. When the amount of subjects was increased from 27 (or 32) to 59 the resulting HTER of the Hotelling's *T*-square test was better than the average between the HTERs produced by the smaller groups. The HTER produced by the Student's *t*-test in the combined dataset case was higher than the HTERs of each individual dataset indicating the lower tolerance of this test to the increase in the number of people.

4.1.5 Receiver Operating Characteristics Curve

Figure 4 presents a Receiver Operating Characteristics

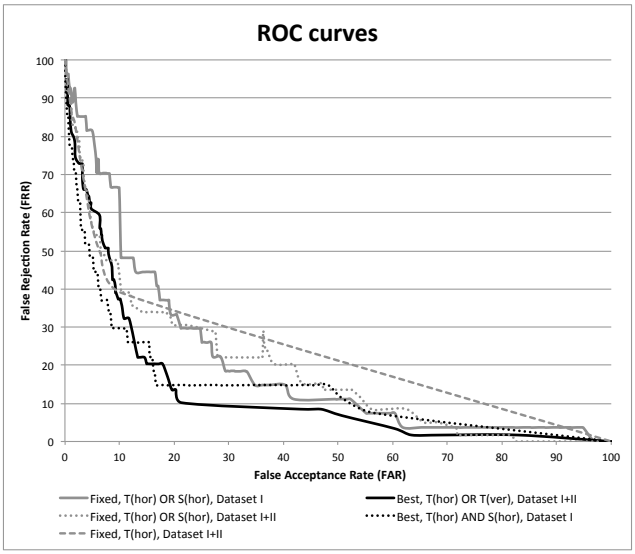

Figure 4: Receiver operating characteristics curves. (ROC) curve. The results include a mix of best performing methods with and without fusion according to the corresponding HTER for the data from Table I.

4.2. "Best" Performance

In general, optimal selection of OPC subset, significance level, and number of votes for the Students *t*-test resulted in improvement of accuracy among all methods, ultimately obtaining the minimum HTER of 19% for *T(hor) OR S(hor)* method. However, general performance trends related to impact of different authentication methods, stimuli, and fusion remained similar to the "Fixed" scenario. The scalability trend was similar to the "Fixed" scenario as well.

5. Discussion

Recording Equipment: The OPC biometrics exploration done in this work was conducted on a very accurate eye tracking equipment with a very high sampling rate. Subjects were positioned in a chinrest to avoid potential signal accuracy issues. Additional research is required to understand the tradeoffs between the authentication accuracy of the OPC biometrics and equipment's sampling rate, positional accuracy, and freedom of head movements.

Stimulus: The jumping dot stimulus employed in this work was purposefully fixed in amplitude and exhibited a large number of jumps. Such fixed experimental parameters allowed establishing a baseline for the OPC biometric performance in an environment that is close to ideal. However, additional work is required to understand the OPC biometric performance for saccades that have randomized amplitudes, various spatial placement, and different quantities.

OPC Estimation Speed: The estimation of an OPC vector containing nine parameters that provided the smallest error between the recorded and simulated saccade required on average 1500 saccade trajectory simulations that took approximately 15 minutes on an Intel Q6600 processor, using one core and assuming MATLAB implementation of the *fminsearch* function. However, the OPC biometrics architecture is highly parallelizable and distributable, with each individual saccade trajectory easily processed by a separate core. Additionally, implementation in a programming language such as C/C++ might speed up the estimation process. It is possible that the reduction in the number of iterations might provide the results comparable to the ones that were obtained; however, such possibility will be explored in the future work.

The linear design of the OPMM makes it possible to seek analytical solutions to the differential equations describing the model, therefore providing an opportunity for the direct extraction of the OPC from saccade trajectories. However the derivation of the analytical solution is very challenging.

Stability of the OPC trait: The time interval between the recording sessions for each subject was approximately 20 min. Such a time difference provides extremely limited insight in terms of the stability of the OPC biometrics over a longer time span and impact of such factors as stress, fatigue, aging and illness. Additional research needs to be conducted to explore the long-term stability of the OPC trait.

Sensitivity of Hotelling's *T*-square Test: The number of subjects employed in this work is 59, which satisfies the sample size requirements for application of the Hotelling's *T*-square Test. However, if larger sample sizes are untenable, the Box test or Box's *M* [29] can be conducted as a precursor to conducting Hotelling's *T*-square. The Box test uses an approximation to the *F*-statistic, and should the test be rejected, a correction can be made to adjust for unequal covariance matrices thereby ensuring accurate hypothesis tests. For example, when applied to the datasets discussed in this paper, the Box test was rejected indicating heterogeneous covariance between subjects (i.e. a lack of tenability of the assumption of compound symmetry). Due to the lack of compound symmetry in covariance matrices between subjects, we compared the results of Hotelling's *T* relative to an adjusted *F*-test (i.e., corrected for non-sphericity). The results were the same and therefore the violation of homogeneity of covariance matrices did not adversely impact the sensitivity of the Hotelling's *T* statistical test employed in this work, indicating that Hotelling's *T*-square Test was the right choice as a matching test for comparison of OPC biometric templates.

6. Conclusion and Future Work

This paper outlined and explored a novel biometrics approach that allows person identification via the internal non-visible anatomical structure of an individual human

eye. Given the limited pool of 59 volunteers, the proposed biometrics method operating in the authentication mode ultimately achieved the lowest HTER of 19% with the optimal sub-set of the oculomotor plant characteristics.

Among statistical methods employed for comparison of ocular templates the multivariate Hotelling's *T*-square test, in general, provided higher accuracy across the nine parameters when compared to the Student's *t*-test, indicating a superiority of multivariate approach to a singular evaluation strategy given the complex nature of the oculomotor plant. Logical fusion methods were able to achieve slightly higher authentication accuracy than when no fusion was performed. An increase in the number of subjects from 27 to 59 did not decrease the authentication performance with the Hotelling's *T*-square test, however when Student's *t*-test was employed the authentication accuracy decreased.

It was concluded that stimuli properties impact the authentication accuracy, i.e., stimulus that evoked large amplitude saccades produced larger authentication errors.

It is important to conduct more work to ensure OPC biometrics independence from equipment calibration biases, because this is one of the main factors degrading accuracy of the authentication performance. In fact our ongoing work includes developing a correction equation for systematic error generated from instrumentation. Additional work should be performed to allow faster estimation of the OPC values. The stability of biometrics needs to be verified against a more diverse array of stimuli, eye tracking equipment, larger group of subjects and a longer time span. To address such issues, we are currently working on a simulation approach using Bayesian probabilistic modeling and Markov chain Monte Carlo methods that will allow us to generate, test and evaluate the OPC biometric performance under a variety of conditions likely to be encountered in real world scenarios of use of our approach.

7. Acknowledgements

This work was partially funded by a grant from the National Institute of Standards #60NANB10D213.

8. References

[1] L. D. Harmon, M. K. Khan, R. Lasch, and P. F. Ramig, "Machine identification of human faces," *Pattern Recognition,* vol. 13, pp. 97-110, 1981.

[2] A. Jain, L. Hong, and Y. Kulkarni, "A Multimodal Biometric System Using Fingerprint, Face, and Speech," in *Proceedings of the International Conference on Audio- and Video-Based Biometric Person Authentication (AVBPA)*, 1999, pp. 182-187.

[3] J. G. Daugman, "High Confidence Visual Recognition of Persons by a Test of Statistical Independence," *IEEE Trans. Pattern Anal. Mach. Intell.,* vol. 15, pp. 1148-1161, 1993.

[4] L. Wiskott, "Face recognition by elastic bunch graph matching," 1997, pp. 129-129.

[5] J. M. Williams, "Biometrics or ... biohazards?," presented at the Proceedings of the 2002 workshop on New security paradigms, Virginia Beach, Virginia, 2002.

[6] K. Hollingsworth, K. W. Bowyer, and P. J. Flynn, "All Iris Code Bits are Not Created Equal," in *Biometrics: Theory, Applications, and Systems, 2007. BTAS 2007. First IEEE International Conference on*, 2007, pp. 1-6.

[7] A. Jain, L. Hong, and S. Pankanti, "Biometric identification," *Commun. ACM,* vol. 43, pp. 90-98, 2000.

[8] U. Park, A. Ross, and A. K. Jain, "Periocular biometrics in the visible spectrum: a feasibility study," presented at the Proceedings of the 3rd IEEE international conference on Biometrics: Theory, applications and systems, Washington, DC, USA, 2009.

[9] P. Kasprowski and J. Ober, "Eye Movements in Biometrics," presented at the Proceedings of the European Conference on Computer Vision (ECCV), 2004.

[10] R. Bednarik, T. Kinnunen, A. Mihaila, and P. Fränti, "Eye-Movements as a Biometric," in *Image Analysis*, ed, 2005, pp. 780-789.

[11] D. R. Wilkie, *Muscle*, 2nd ed.: London: Arnold, 1970.

[12] O. Komogortsev, V. and J. Khan, "Eye Movement Prediction by Kalman Filter with Integrated Linear Horizontal Oculomotor Plant Mechanical Model," in *ACM Eye Tracking Research & Applications Symposium*, Savannah, GA, 2008, pp. 229-236.

[13] O. V. Komogortsev, D. V. Gobert, S. Jayarathna, D. Koh, and S. Gowda, "Standardization of Automated Analyses of Oculomotor Fixation and Saccadic Behaviors," *IEEE Transactions on Biomedical Engineering,* vol. 57, pp. 2635-2645, 2010.

[14] O. V. Komogortsev and U. K. S. Jayarathna, "2D Oculomotor Plant Mathematical Model for eye movement simulation," in *IEEE International Conference on BioInformatics and BioEngineering (BIBE)*, 2008, pp. 1-8.

[15] J. C. Lagarias, J. A. Reeds, M. H. Wright, and P. E. Wright, "Convergence Properties of the Nelder--Mead Simplex Method in Low Dimensions," *SIAM Journal on Optimization,* vol. 9, pp. 112-147, 1998.

[16] C. C. Collins, "The human oculomotor control system," *Basic Mechanisms of Ocular Motility and Their Applications,* pp. 145-180, 1975.

[17] C. Collins, "Orbital mechanics," in *The Control of Eye Movements*, P. Bach-y-Rita and C. Collins, Eds., ed New York: Academic, 1971.

[18] B. J. Winer, D. R. Brown, and K. M. Michaels, *Statistical Principles in Experimental Design*: McGraw-Hill, 1991.

[19] H. Hotelling, "The Generalization of Student's Ratio," *The Annals of Mathematical Statistics,* vol. 2, pp. 360-378, 1931.

[20] L. Lam and S. Y. Suen, "Application of majority voting to pattern recognition: an analysis of its behavior and performance," *IEEE Transactions on Systems, Man and Cybernetics, Part A: Systems and Humans,* vol. 27, pp. 553-568, 1997.

[21] K. Ito and W. J. Schull, "On the robustness of the T02 test in multivariate analysis of variance when variance-covariance matrices are not equal," *Biometrika,* vol. 51, pp. 71-82, June 1, 1964 1964.

[22] A. A. Ross, K. Nandakumar, and A. K. Jain, *Handbook of Multibiometrics*: Springer, 2006.

[23] J. Daugman. (2000). *Combining Multiple Biometrics*. Available: http://www.cl.cam.ac.uk/~jgd1000/combine/combine.html

[24] EyeLink. (2010). *EyeLink II*. Available: http://www.sr-research.com/EL_1000.html

[25] O. V. Komogortsev. (2011). *Eye Movement Biometric Database v1*. Available: http://www.cs.txstate.edu/~ok11/embd_v1.html

[26] R. J. Leigh and D. S. Zee, *The Neurology of Eye Movements*: Oxford University Press, 2006.

[27] R. J. Harris, *A Primer of Multivariate Statistics*. Mahwah, NJ: Lawrence Erlbaum Publishers, 2001.

[28] N. Balakrishnan and V. B. Nevzorov, *A Primer on Statistical Distributions*. New York, NY: John Wiley & Sons, 2003.

[29] G. E. P. Box, "A General Distribution Theory for a Class of Likelihood Criteria," *Biometrika,* vol. 36, pp. 317-346, 1949.